IOSR Journal of Applied Geology and Geophysics (IOSR-JAGG)
e-ISSN: 2321–0990, p-ISSN: 2321–0982.Volume 3, Issue 6 Ver. I (Nov. - Dec. 2015), PP 33-45
www.iosrjournals.org

Edge Detectionand Depth Estimation from Magnetic DataofWadi Araba,Eastern Desert- Egypt.

Saada Ahmed Saada
Geology Department, Faculty of Science, Suez University, Suez, Egypt,

Abstract: *Edge detection, trend analysis and depth estimation techniques are very important steps in the interpretation of magnetic anomalies. In this paper, the Fast Fourier Transform was applied to showing the regional and residual sources. Trend analysis was carried out on the Reduced to Pole, regional and residual aeromagnetic maps to delineate the main tectonic trends dissected the study area. The edges of these sources is determined by using the tilt angle derivative and standard 3D-Euler deconvolution. The estimated Euler solutions was plotted on the tilt angle derivative map. A good correlation was noticed between them indicating that both of them can be contribute in delineating the general structural framework of the area. These techniques indicate that Wadi Araba is highly affected by the Gulf of Suez rifting system and the Syrian Arc folding system. On other hand, the area is affected by the Tethyan trend especially the southwestern corner of this area and it is maintained in regional components. The depth estimation was applied using analytic signal and Source Parameter imaging techniques. These depth methods show a comparable results. The depth to the top of the basement sources ranges from about 200 to 4000 m.*

Keywords: *Wadi Araba, Galala, FFT, Edge Detection, TDR, ED, AS and SPI.*

I. Introduction

[1] and [2] describe edge detection of causative sources as one of the most important stages in the modelling of both magnetic and gravity anomalies. Severaltechniques that have been involved to recognize edge detection, for example, Analytic signal (AS), tilt angle derivative (TDR), Euler Deconvolution (ED) and etc. [3]. The potential field derivatives are largely used to modelling the buried sources [3]. [4], [5], [6] and others used theAS to interpret andmodel bothgravity and magnetic data.

The magnetic data is related to changes in magnetic susceptibilities and depths of their sources. So, these data are used to determining the location and the depth of the magnetic bodies that caused these data. This aim has recently become particularly important because of the abundance of magnetic data that wasapplied for reconnaissance explorations of minerals and petroleum. Different methods, based on the use of derivatives of the magnetic field, have been developed to determine magnetic source parameters such as locations of boundaries and depths [7]. [8] used Source Parameter Imaging (SPI) to determine the depth to basement.

In this paper, the Fast Fourier Transform (FFT) is used to separating the regional and residual components. Trend analysis was applied to determine the main trends of these component. Different derivative techniques (e.g., TDR and ED) werecarried out on Wadi Araba to locate the boundaries and the depths of different magnetic sourcesas well as their trends. It is interested to correlate between these edge detection methods to measure the degree of similarity between their results. AS and SPI are used to estimate the depth to basement of the study area.

II. The Study Area

Since Turonian times, the area of the Galala Mountains was influenced by vertical movementsof the Syrian Arc fold belt, marking the initialstages of the collision between the African andEuropean plates [9]. Asconsequence, in northern Egypt and Sinai a system of inverted, uplifted and folded grabbenswas formed along the Syrian Arc in Egypt also is known as the unstable shelf [10]. As a consequence of the uplift of theNorthern Galala/Wadi Araba High, the SouthernGalala Sub-basin evolved further south, forminga part of the Eastern Desert Intrashelf Basin[11].During the uplift of the Northern Galala/ Wadi Araba High, successively older sediments were exposed and subsequently eroded [12]. During Oligocene and Miocene ages, the Study area was affected by the Gulf of Suez rifting system.

So, Wadi Araba has an ENE (Syrian Arc) trend direction. It separates the Northern and the Southern Galala Plateaus (Galala El Bahariya from Galala El Qibliya).It is the most important wadis (dry valleys) in the northern part of the north Eastern Desert. The area under investigation lies on the northern part of Egyptian Eastern Desert. It lies on the western side of the Gulf of Suez and covers a surface area of about 2,300 km^2 (Fig. 1). Nearly, it coversWadi Araba and the southern part of GalalaEl Bahariya Plateau as well as the northern part of Galala El Qibliya. An ENE sharp slope is shown along Monastery of St. Antony and Gebel Thelemet area (Fig. 1) in the southern part. Wadi Araba, like other localities in the northern part of the Eastern Desert, is

affected by volcanic intrusions. Basalt sheets can be seen at the top of the plateau, and also at several opening of its valleys.

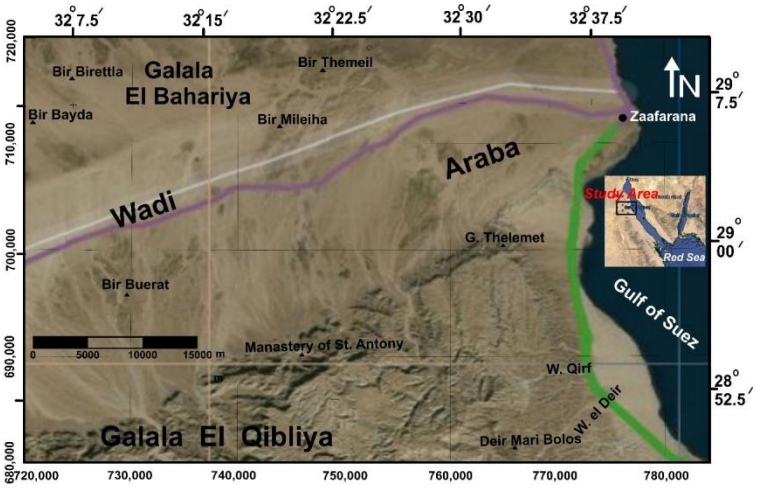

Fig. 1: Location map of Wadi Araba El Bahariya Plateau.

The complexity of the structure of the area is tightly related to the regional structures in the north Eastern Desert. According to [13], the main structural elements show three types primary, secondary structures and Dikes.

The first one including the flow structure, Beading, lamination, Graded Bedding and unconformities. While the second one has a sheeting, foliation, fracture cleavage, folds, joints and faults. The third type of structural elements, dikes, which cutting the area. These dikes include three types, acidic, intermediate and finally basic dikes.

Folding plays a minor role in controlling the structural pattern of the western Gulf of Suez area. Most of the noticed folds were either produced by bending of the strata before breaking or by movements caused the less rigid sediments, especially the Miocene sediments, to bend in anticlinal or synclinal folds [10].

III. Data Source

Aeromagnetic surveys in Egypt flown in the 1983. The magnetic data are digitized from total intensity magnetic map with scale of 1:50,000 after the Egyptian General Petroleum Corporation [14].It was surveyed at a flight direction of 45/225º& tie 135/315º, flight altitude 120m terrain clearance, flight interval 1.5km traverse & tie 10km, inclination angle 39.5º N and declination angle of 2º E, the total magnetic intensity 42425nT and contour interval of 2nT. The total intensity aeromagnetic map is shown in Fig. (2). The reduced to pole (RTP) map (Fig. 3) is construct using [15]. This step is applied to correct the position of the magnetic anomalies directly above their true sources.

IV. Methodology

4.1 Regional- Residual separation using the Fast Fourier Transform (FFT)

The Fast Fourier Transform (FFT) was applied on the magnetic data for calculating the energy spectrum curves and estimating the residual (shallow) and regional (deep) sources. This filter is based on the cut-off frequencies that pass or reject certain frequency values and pass or reject a definite frequency band.

Radially averaged power spectrum method is used to determine the depths of volcanic intrusions, depths of the basement complex and the subsurface geological structures. Several authors, such as [16] and [17] explained the spectral analysis technique. It depends on the analysis of the magnetic data using the Fourier Transform. It is a function of wavelengths in both the X and Y directions. The grid is processed to become periodic on its edges. The Fourier transform $f(\mu, y)$ of periodic function $f(x, y)$ is given by [18]as:

$$f(\mu,\gamma) = \int_{-\infty}^{+\infty}\int_{-\infty}^{+\infty} f(x,y).e^{-i(\mu x+\gamma y)}\,dx.\,dy \quad \ldots\ldots (1)$$

Where:

(x) and (y): are the spatial coordinates in the x and y directions respectively

γ and μ : are the angular frequencies in the x and y directions respectively.

4.2 Edge detection methods

4.2.1 The tilt angle derivative (TDR)

TDR is used for mapping shallow basement structures and mineral exploration targets [15].TDR is used for enhancing features and causative body edge detection in potential field images. [19] and [20] suggested the tilt angle filter. It was developed later by others such [21], [7] and [22]. It showed a considerable interest because of its fundamental and practical simplicity [23]. This filter is defined as:

$$T\text{DR} = \tan^{-1}\left(\frac{VDR}{THDR}\right) \quad \text{…….. (2)}$$

Where VDR is the vertical derivative and THDR is the total horizontal derivatives.

i.e.: $$T\text{DR} = \tan^{-1}\left(\frac{\partial f / \partial z}{\sqrt{(\partial f / \partial x)^2 + (\partial f / \partial y)^2}}\right) \quad \text{…… (3)}$$

Where f is the magnetic or gravity field and $\delta f/\delta x$, $\delta f/\delta y$ and $\delta f/\delta z$ are the first derivatives of the field f in the x, y and z directions. The amplitudes of TDR range between $-\pi/2$ to $+\pi/2$ (radian) or -90º-90º regardless of the amplitude of the vertical derivative or the absolute value of the total horizontal gradient [7]. The TDR produces a zero value over or close to the source edges and, therefore, can be used to trace the outline of the edges [19]. Positive values are located directly above the sources while negative values is located away from them. Furthermore, the horizontal distance from the 45º to the 0º position of the tilt angle is equal to the depth to the top of the contact [23] or the half distances between -45º to +45º [21].

4.2.2Standard 3D-Euler Deconvolution (ED)

Recently, use of this method has become more widespread because it has been automated and rapid interpretation that work with either profile or grid data ([24], [25], [26], [27], [28] and [29]).

It requires three orthogonal gradients (two horizontal and vertical gradients) of the magnetic or gravity data, which (if they have not been measured) are normally, calculated using FFT. Hence, it is normally applied to gridded data, where the data-sampling interval is uniform. It passes a moving window through the data, and uses least-squares inversion to obtain the depth and horizontal location of sources with different structural indices. ED technique was introduced in the potential field data to estimate the position of structural lineament. In this technique no prior source magnetization direction required and does not affect by the presence of remanence [30]. Usually the structural index (SI) is fixed and the locations and depths (x_0, y_0, z_0) of any sources are found using the following equation (4):

$$\frac{\partial f}{\partial x}(x - x_0) + \frac{\partial f}{\partial y}(y - y_0) + \frac{\partial f}{\partial z}(z - z_0) = SI(\text{B} - f) \text{ ..... (4)}$$

Where f is the observed field at location (x, y, z) and B is the base level of the field (regional value at the point (x, y, z)) and SI is the structural index or degree of homogeneity [24]. The equation is solved for the source position by least-squares inversion of a moving window of data points. To obtain an accurate estimate of the source locations, the field data used must adequately sample the anomalies present in the data.

Accordingly, ED requires four sets of grids as input data; the total magnetic field, first horizontal derivative in x, y and vertical derivative in z-direction. It is insensitive to magnetic inclination and declination. So, the north-south extending geologic features reflect a low signal to noise ratio in the data and therefore, reduction to the pole data can be applied to improve this situation [31]. The size of window (cell size) should be chosen large enough to incorporate substantial variation of the field gradients and it should be small enough not to include significant effects from multiple sources. I.e. the board anomalies arising from deep sources are poorly represented in small windows and vice versa. The quality of depth estimation depends on the choice of the correct structural index and adequate sampling of data. So, the choice of the SI and electing of optimum criteria for selecting solutions are fundamental requirements for successful application of this method.

4.3 Depth to basement estimation

4.3.1 Analytic signal (total gradient) method

The analytic signal (AS) is the square root of the sum of the squares of the derivatives in the x, y and z directions as illustrated by equation (5):

$$\text{AS} = \sqrt{\left(\frac{\partial f}{\partial X}\right)^2 + \left(\frac{\partial f}{\partial Y}\right)^2 + \left(\frac{\partial f}{\partial z}\right)^2} \quad \text{……. (5)}$$

Where $\frac{\partial f}{\partial x}, \frac{\partial f}{\partial y}$ and $\frac{\partial f}{\partial z}$ are the first derivative of the total magnetic field. It is very useful in locating the edges of magnetic source bodies [15]. The advantage of using AS techniques to determine magnetic parameters from magnetic anomalies is the independence of magnetization direction (inclination). A drawback of this method, however, is the assumption that near-surface structures can be characterized adequately by step models. To improve mapping resolution, the amplitude ratio method has been extended to comprise both step-like and dike-like structures. A criterion is constructed that discriminates between maxima from dike-like or step-like structures and significantly improves near-surface structural mapping. This avoids a bias in geological interpretation caused by the original assumption that all structures can be characterized by step models ([32] and [33]).

The success of the AS method results from the fact that the location and depth of magnetic sources are found with only a few assumptions about the natural of the source body, which is usually assumed as 2D magnetic source (for example, step, contact, horizontal cylinder and dike). For these geological models, the shape of the amplitude of the AS is a bell-shaped symmetric function located directly above the source body. The magnetic sources depths using the magnetic method are estimated from the ratio of the total magnetic AS to the vertical derivative analytic signal (AS1) of the total magnetic field as shown in equations (6) and (7).

$$\mathrm{AS1} = \sqrt{\left(\frac{\partial fv}{\partial X}\right)^2 + \left(\frac{\partial fv}{\partial Y}\right)^2 + \left(\frac{\partial fv}{\partial z}\right)^2} \quad \ldots\ldots (6)$$

On the maximum amplitude

$$\mathrm{D} = \frac{\mathrm{AS}}{\mathrm{AS1}} \times N \quad \ldots\ldots (7)$$

Where fv is the first vertical derivative of the total magnetic field, and D is the depth to the magnetic body, N is known as a structural index and is related to the geometry of the magnetic source. For example, N=4 for sphere, N=3 for pipe, N=2 for thin dike and N=1 for magnetic contact [24].

4.3.2 Source Parameter Imaging (SPI) Technique (local wavenumber technique)

SPI is a technique based on the extension of complex AS to estimate magnetic depths, it is also known as local wavenumber. The original SPI method [34] works for two models: a 2-D sloping contact or a 2-D dipping thin-sheet. For the magnetic field f, the local wavenumber is given by equation (8):

$$k = \frac{\frac{\partial^2 f}{\partial x \partial z}\frac{\partial f}{\partial x} - \frac{\partial^2 f}{\partial x^2}\frac{\partial f}{\partial z}}{\left(\frac{\partial f}{\partial x}\right)^2 + \left(\frac{\partial f}{\partial z}\right)^2} \quad \ldots.. (8)$$

For the dipping contact, the maxima of k are located directly over the isolated contact edges and are independent of the magnetic inclination, declination, dip, strike and any remnant magnetization. The depth is estimated at the source edge from the reciprocal of the local wavenumberi.e.:

$$Depth_{(x=0)} = \frac{1}{k_{\max}} \quad \ldots.. (9)$$

Where K_{max} is the peak value of the local of number K over the step source.

One more advantage of this method is that the interference of anomaly features is reducible, since the method uses the second-order derivatives. The SPI computes source parameters from gridded magnetic data. Solution grids show the edge locations, depths, dips, and susceptibility contrasts. The estimate of the depth is independent of the magnetic inclination, declination, dip, strike and any remanent magnetization [34].

In practice, the method is used on gridded data by first estimating the direction at each grid point. The vertical gradient is computed in the frequency domain, and the horizontal derivatives are computed in the direction perpendicular to the strike using the least-squares method.

V. Results And Discussion

The shaded colored relief of the total intensity aeromagnetic map (Fig. 2) shows two high positive anomalies in the southeastern cornerand in the northern portion which distributed around Wadi Araba. These anomalies istrending in the NW direction. The negative anomalies are located along Wadi Araba with different

trends, amplitudes and gradient. An alternative positive and negative sharp anomalieswith small extensiontrending in the NW direction are shown in the eastern part. The maximum magnitude (42427nT) is recorded in the northern partclose to Bir Mileiha.

The RTP map (Fig. 3) shows that the main positive and negative anomalies are shifted to the north. The maximum positive anomaly with a magnitude of 171nT (after removing the main field of 42325 nT) is located in the southern part. Sharp anomalies with small extension can be noticed running from Monastery of St. Antony to Bir Birttla and Bir Bayda. This may be due to shallow basement structures. Generally, the RTP magnetic map is used to carrying out different analytical techniques applied in this study.

The average energy power spectrum (Fig. 4) for the RTP aeromagnetic data of the studied area was applied using Geosoft Program [15]. This figure indicates that the depth to the source bottom is not recorded where a maximum peak is not represented [23]. From the power spectrum curve the regional and residual as well as noise signals are determined. The corresponding depth estimate chart is used to calculating the average depths to the top of these deep and shallow sources. The calculated average depth to the top of regional sources is about 4 km whereas the shallow sources has a depth of about 1.5 km as an average depth to their sources (Fig. 4).

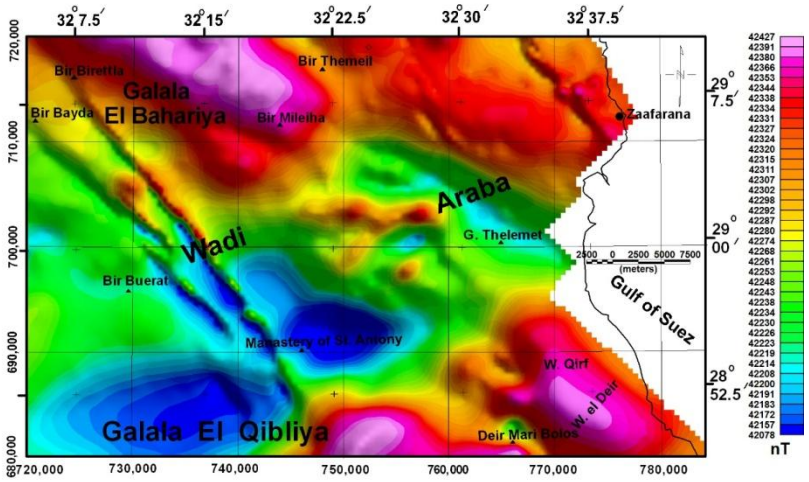

Fig. 2: Shaded color total intensity aeromagnetic map of Wadi Araba.

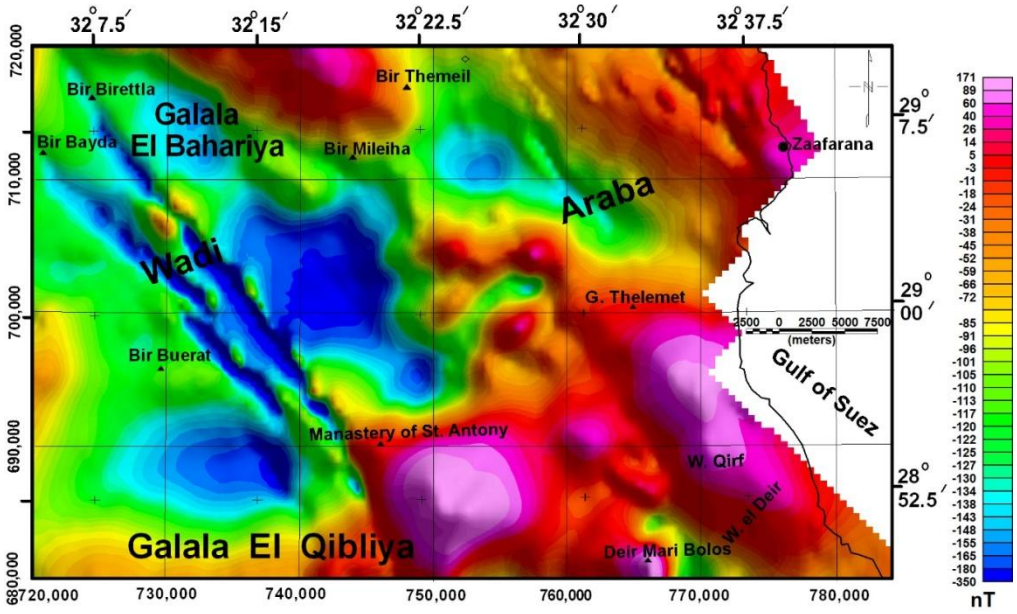

Fig. 3: Shaded color RTP aeromagnetic map of the Wadi Araba

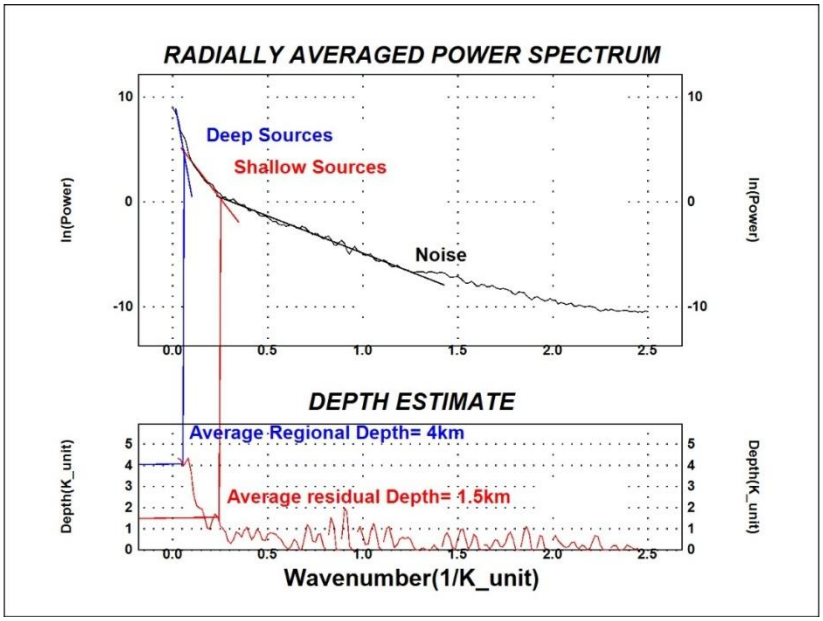

Fig. 4: Power spectrum of aeromagnetic data showing the corresponding average regional and residual depths, Wadi Araba area.

According to this chart a low- and high-passes maps are constructed. The low-pass map (Fig.5) is constructed with a cut-off wavelength of 13333 m (wavenumber 0.075Rad/km). It shows a NW (Suez) trend affecting the eastern parts of the study area while the western parts is more affected by the E-W (Tethyan) trend. On other hand, the high-pass filtered map (Fig. 6) exhibits a NW (Gulf of Suez) and NE to ENE trends allover the area. TheE-W trend completely absent. On this map we can see alternative closed elongated positive and negative anomalies has a NW trend. From the regional and residual maps we can conclude that the older E-W trend was intersected by younger NW and ENE to NE trends [35]. The eastern parts of the area along the Gulf of Suez was affected by the Gulf of Suez Rifting system during Miocene. The NW faults (oriented parallel to the Gulf of Suez) Wadi Araba are also aligned with major basement lineaments and may have exploited preexisting basement structures during rifting time [36].

Trend Analysis:

The main purpose of using the two dimensional trend analysis technique is to define statistically the tectonic trends developed in the area. A simple and standard method for portraying the two dimensional patterns is to construct a frequency plot, showing the percentage of trends lying in various direction ranges. The magnetic provinces of consistent magnetic character can define a tectonic unit ([37] and [38]).

Using Affleck's technique [37], different trends are determined for the RTP, the low-pass (regional) and high-pass (residual) filtered magnetic maps. The determined trends are counted and measured (Azimuth and Length). They were studied statistically to calculate their number and length percentages (N % and L %) as well as the number to length ratio (Tables 1, 2 and 3).

For rapid visual inspection, different magnetic trends are represented in a frequency curve (Fig. 7) by their length percentage (L %) distribution. They clearly show four major peaks that trend in N35-45°W (Suez), N65°W (Najd), N85°W to N85°E (Tethyan) and N45-60°E (Syrian Arc), arranged in decreasing order of magnitude. The N85°W to N85°E (Tethyan or Mediterranean) trend appears as the second order of magnitude for the regional map (after the Gulf of Suez trend) but it comes as the last order of magnitude for the residual map.

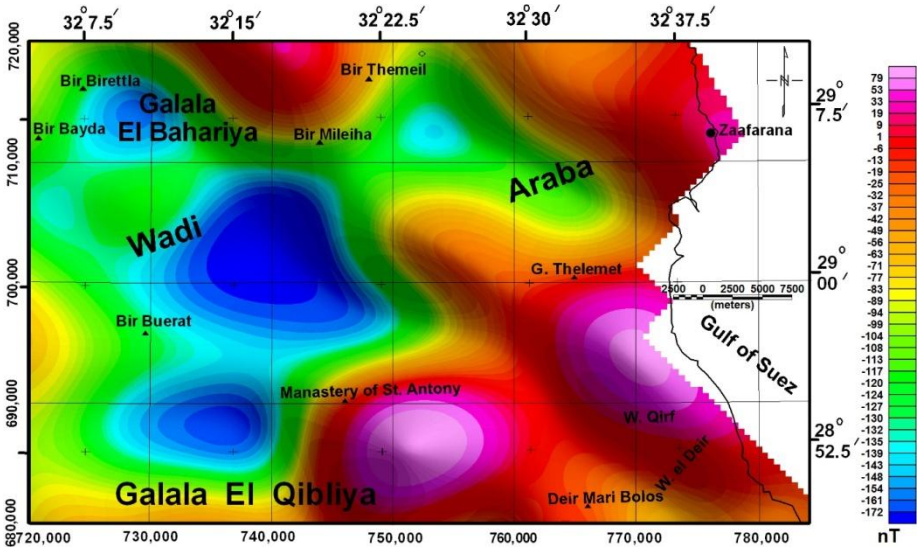

Fig. 5: Shaded color map of the RTP regional (low-pass) magnetic- component, Wadi Araba area.

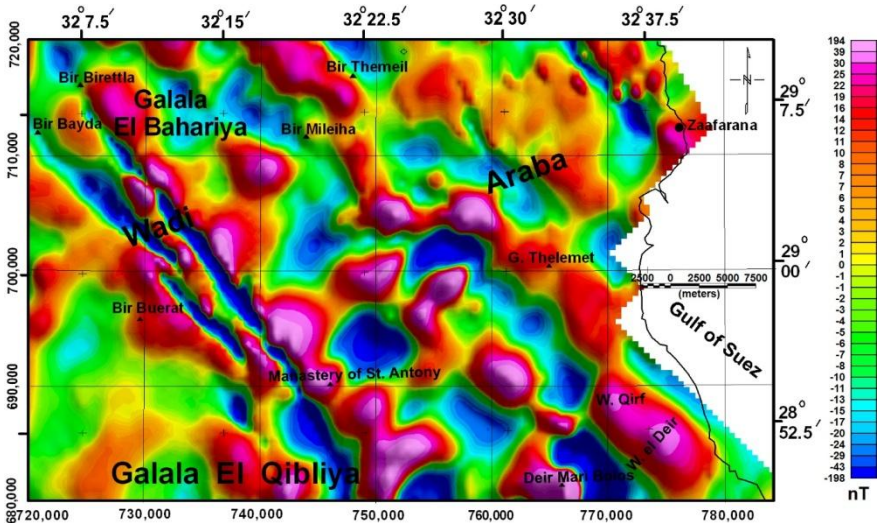

Fig. 6: Shaded color map of the RTP residual (high-pass) magnetic- component, Wadi Araba area.

The most prevailing magnetic trends are more or less parallel to the trend of Gulf of Suez. These tectonic trends are familiar trends in the basement rocks of Gulf of Suez and the north Red Sea areaswere discussed by many authors e.g.[10], [39], [40], [41], [42], [43] and others.

Table (1): Parameters of the major fault trends detected from RTP magnetic map.

WEST					Azimuth	EAST				
N	N%	L	L%	L/N		L/N	L%	L	N%	N
5.0	8.9	19.8	4.9	4.0	0:<10	2.5	1.2	5.0	3.6	2.0
4.0	7.1	11.0	2.7	2.8	10:<20	4.6	3.4	13.9	5.4	3.0
5.0	8.9	26.9	6.6	5.4	20:<30	E	0.0	0.0	0.0	0.0
3.0	5.4	53.9	13.2	18.0	30:<40	5.5	1.4	5.5	1.8	1.0
10.0	17.9	108.3	26.6	10.8	40:<50	5.4	2.6	10.7	3.6	2.0
4.0	7.1	38.5	9.4	9.6	50:<60	0.0	2.6	10.5	5.4	3.0
4.0	7.1	40.9	10.0	10.8	60:<70	E	0.0	0.0	0.0	0.0
2.0	3.6	10.4	2.6	0.0	70:<80	5.1	3.7	15.2	5.4	3.0
0.0	0.0	0.0	0.0	5.4	80:<90	0.0	9.1	37.1	8.9	5.0
37.0	66.1	309.7	76.0		Sum		24.0	97.8	33.9	19.0

∑n= 56 ∑L= 407.6 ∑L%= 100%∑n%= 100%

Table (2): Parameters of the major fault trends detected from Regional magnetic map.

WEST					Azimuth	EAST				
N	N%	L	L%	L/N		L/N	L%	L	N%	N
0.0	0.0	0.0	0.0	E	0:<10	6.6	2.4	6.6	4.8	1.0
0.0	0.0	0.0	0.0	E	10:<20	E	0.0	0.0	0.0	0.0
1.0	4.8	3.3	1.2	0.0	20:<30	E	0.0	0.0	0.0	0.0
2.0	9.5	21.9	7.9	11.0	30:<40	6.5	2.4	6.5	4.8	1.0
4.0	19.0	56.6	20.5	14.2	40:<50	8.7	3.1	8.7	4.8	1.0
3.0	14.3	44.3	16.0	14.8	50:<60	E	0.0	0.0	0.0	0.0
2.0	9.5	39.2	14.2	19.6	60:<70	E	0.0	0.0	0.0	0.0
1.0	4.8	20.4	7.4	20.4	70:<80	E	0.0	0.0	0.0	0.0
3.0	14.3	50.0	18.1	16.7	80:<90	9.6	6.9	19.2	9.5	2.0
16.0	76.2	235.7	85.2		Sum		14.8	41.0	23.8	5.0

∑n= 21 ∑L= 276.7km ∑L%= 100%∑n%= 100%

Table (3): Parameters of the major fault trends detected from Residual magnetic map

WEST					Azimuth	EAST				
N	N%	L	L%	L/N		L/N	L%	L	N%	N
6.0	6.3	26.0	4.4	4.3	0:<10	3.0	1.5	9.1	3.2	6.0
5.0	5.3	14.9	2.5	3.0	10:<20	6.3	3.2	19.0	3.2	3.0
11.0	11.6	71.4	12.1	6.5	20:<30	5.0	5.1	30.1	6.3	11.0
16.0	16.8	145.1	24.7	9.1	30:<40	5.8	2.9	17.3	3.2	16.0
15.0	15.8	120.5	20.5	8.0	40:<50	4.7	6.4	37.6	8.4	15.0
5.0	5.3	37.4	6.4	7.5	50:<60	2.4	0.4	2.4	1.1	5.0
2.0	2.1	15.2	2.6	7.6	60:<70	5.8	2.0	11.6	2.1	2.0
0.0	0.0	0.0	0.0	E	70:<80	2.7	1.4	8.0	3.2	0.0
3.0	3.2	13.4	2.3	4.5	80:<90	3.2	1.6	9.5	3.2	3.0
63.0	66.3	443.8	75.4		Sum		24.6	144.7	33.7	61.0

∑n= 124 ∑L= 88.5km ∑L%= 100% ∑n%= 100%

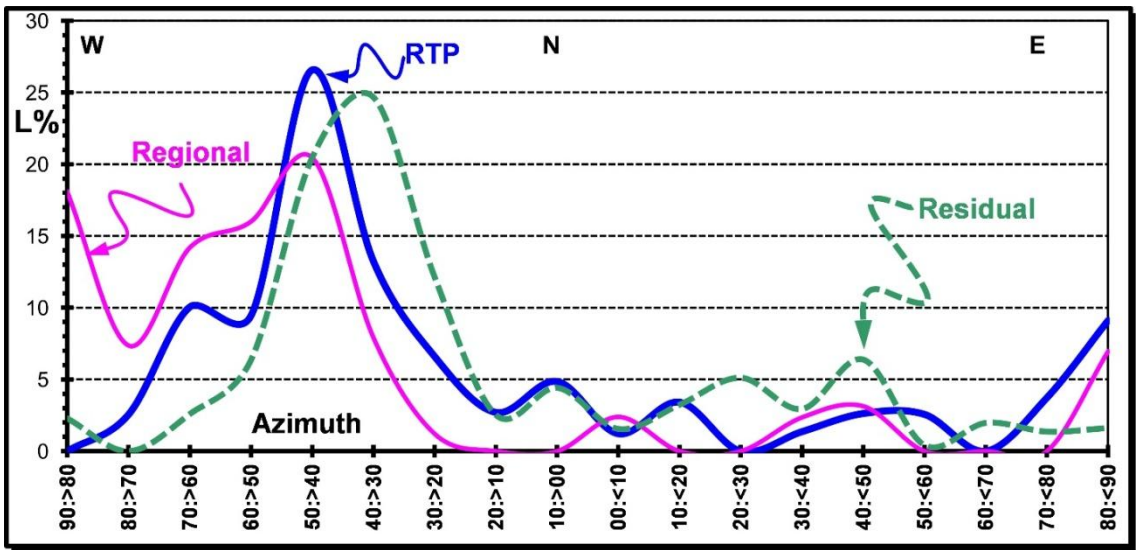

Fig. (7): Frequency distribution curves of the magnetic tectonic trends.

The TDR analysis of Miler and Singh[19] (Fig. 8) shows the geologic features like faults which are depicted as magnetic lineaments. This method facilitates the horizontal location with extent of edges. It is suggested that the zero contour line (the dashed black line) in the TDR map is the location of abrupt changes in magnetic susceptibilities between positive and negative anomalies that is particularly at the sharp gradient. So,

the zero contour line represent the contact boundary of magnetic sources. Zero contours can be identified as light yellow color which is separating the green color (negative values) and red colors (positive values) can be seen from the color scale bar (Fig. 8). On other hand, positive values are assumed to be located directly above these magnetic sources while negative values are locatedaway from them. The TDR of RTP field data shows NW lineament trend allover the study area except for the southwestern corner which reflects an E-W and a NNE trends (Fig. 8).

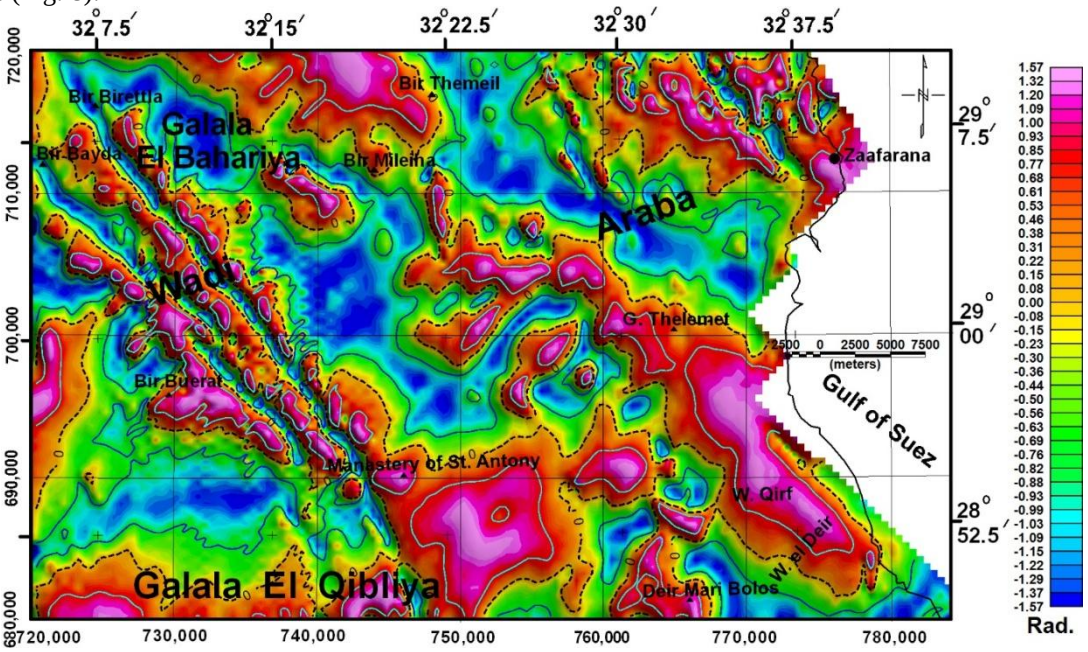

Fig. 8: Shaded color map of the TDR. The black dashed bold line shows the 0 radian contour of the tilt angle while blue and gray solid lines show the $-\pi/4$ and $+\pi/4$ radian contour lines, respectively.

It can be concluded that the structure pattern of the eastern parts of Wadi Araba area along Gulf of Suez was affected by the Gulf of Suez and Red Sea rifting system, as deduced from the TDR map.On other hand, the southwestern part was less affected and still preserves the older E-W (Tethyan or Mediterranean) trend in their basement rocks. Both the NW and the E-W trends form uplifted and down faulted blocks where alternative positive and negative elongated anomalies are represented.

Salem et al. [21] have shown that half-distance between $\pm 45^{o}$ contours provide an estimate of the source depth for vertical contacts. [44]also used the half distance between $\pm\pi/4$ radians ($\pm 45^{o}$) contours to estimate the depths of the edges of the uplifts. Depending on this methods, the depth to the uplifted blocks (the distance between the gray and blue lines) of the study area ranges from few hundreds of meters along Manastery of St. Antony to Bir (well) Birettla area at the western part to more than 4000m at the southern and eastern areas.

Euler depth solution map is shown in Fig. (9). In this work, thestandard3D-ED technique is applied on the RTP aeromagnetic data of Wadi Araba. The window size used is 15x15 (grid cell size =300m) with a maximum depth tolerance of 15%. The structural index used is 0 to locate and determine the contact depth. The calculated depths solutions range from 161m to 4356m. The resulted solutions are plotted on the TDR map as shown in Figure (9) to measure the degree of similarity between them. A very good correlation can be seen by the superposition of solutions to seem as black line over the zero contour TDR dashed line.The main trends of EDsolutions are NW (Suez), WNW (Najd) and E-W as well as ENE (Syrian Arc). These trends can be noticed by the source point'sconcentration as the structural lineaments.

Under the assumption that the edges of anomalous sources are caused by vertical contacts, a very good correlation also is shown between Euler solution locations for magnetic contact and the TDR zero line (Fig. 9). So, both the TDR and ED are good edge (contact) detector and very well correlated among each other for aeromagnetic data.

The basement depth calculations are carried out in the study area by using the AS and source parameter imaging. As mention above, the AS was applied on the RTP aeromagnetic data of Wadi Araba (Fig.10a). It shows the edges locations of the magnetic sources in both horizontal and vertical dimensions. The first vertical derivative (Fig. 10b) shows alternative positive and negative anomalies trending in the NW direction the eastern portion of the area with sharp gradient. The positions and trends of these anomalies are similar to those of the TDR map (Fig. 8). In the AS of the first vertical derivative (AS1) map (Fig. 10c), the NW (Gulf of Suez) trend has the maximum amplitudes.

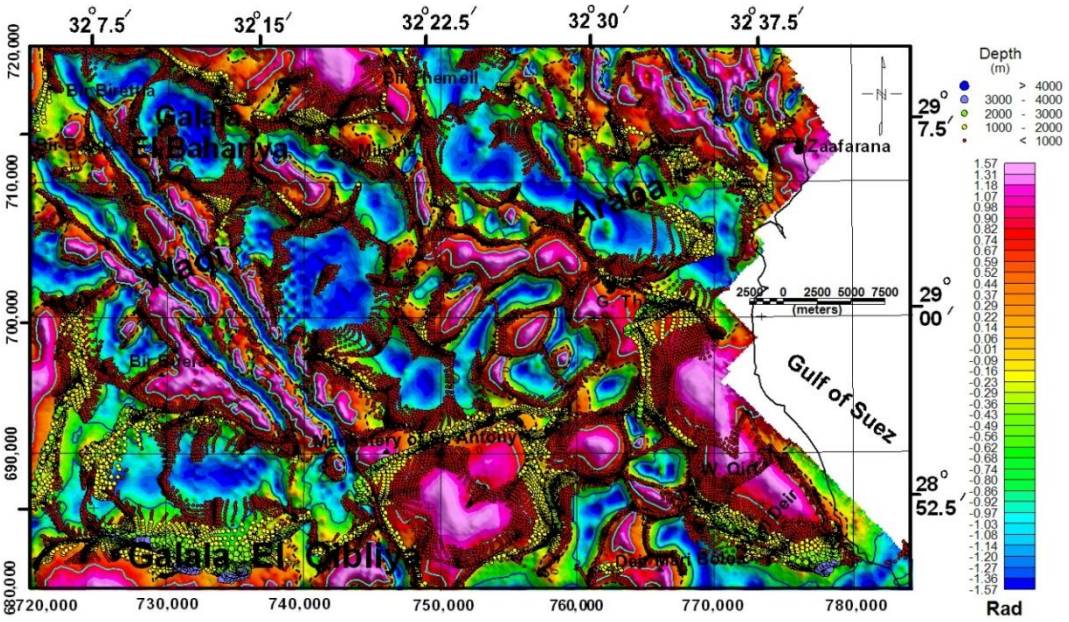

Fig. 9: 3D- Euler solutions plotted on Shaded color map of the TDR, Wadi Araba. N.B. Euler solusions are located on Zero radian contour line of TDR map.

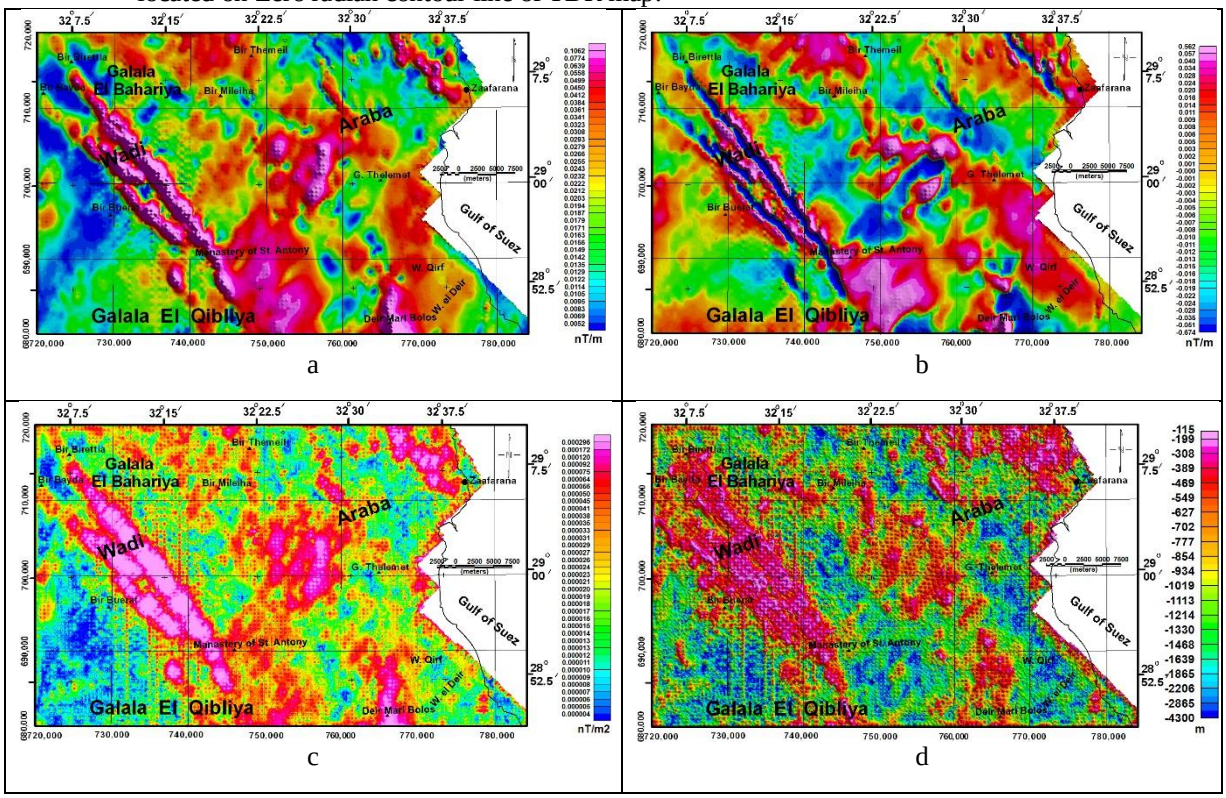

Fig.10:a) Analytic signal, b) First vertical derivative and c) Analytic signal of first vertical derivative shaded color maps used to calculate d) basement depth map.

The AS of the RTP aeromagnetic map (Fig. 10a) is divided by the AS1 map(Fig. 10c) to construct the depth to basement contact of the area (Fig. 10d). Generally, the depth ranges from about 115 0 at the western part north to Bir Buerat to about4300 m at different parts as shown in Figure (10d).Generally, the basement depth map shows three highs alternative with three lows trending in the NW directions. The calculated shallow depths allover the area can be related to the volcanic intrusions and/or dikes which are seen along Wadi Araba and on the top of both Northern and Southern Galala plateaus.

The SPI depth map (Fig. 11) shows great similarity to the depth map constructed by using AS technique. However, the depth ranges from about 200 m to more than3100 m.

VI. Summary And Conclusions

The aeromagnetic data of Wadi Araba are used to detect and locate the edges of the magnetic sources of this area. In order to better interpretation of these sources edges locations and depths estimation, the FFT technique was applied to separating the residual components from the regional ones. The regional sources have an average depth of about 3.75km. On other hand, shallow sources shows average depth of about 1.2 km. The regional sources have an elongated structural pattern trending in the NW and E-W directions while residual sources exhibits an obvious NW and ENE trends allover the study area.

Trend analysis is applied on the RTP, Regional and Residual magnetic maps to illustrate different trends that affected the study area. It shows four main trends which are Suez, Najd, Tethyan and Syrian Arc, arranged in their decreasing order of magnitude. The Tethyan or Mediterranean trend shows more effect on the regional map but has small effect on the residual one.

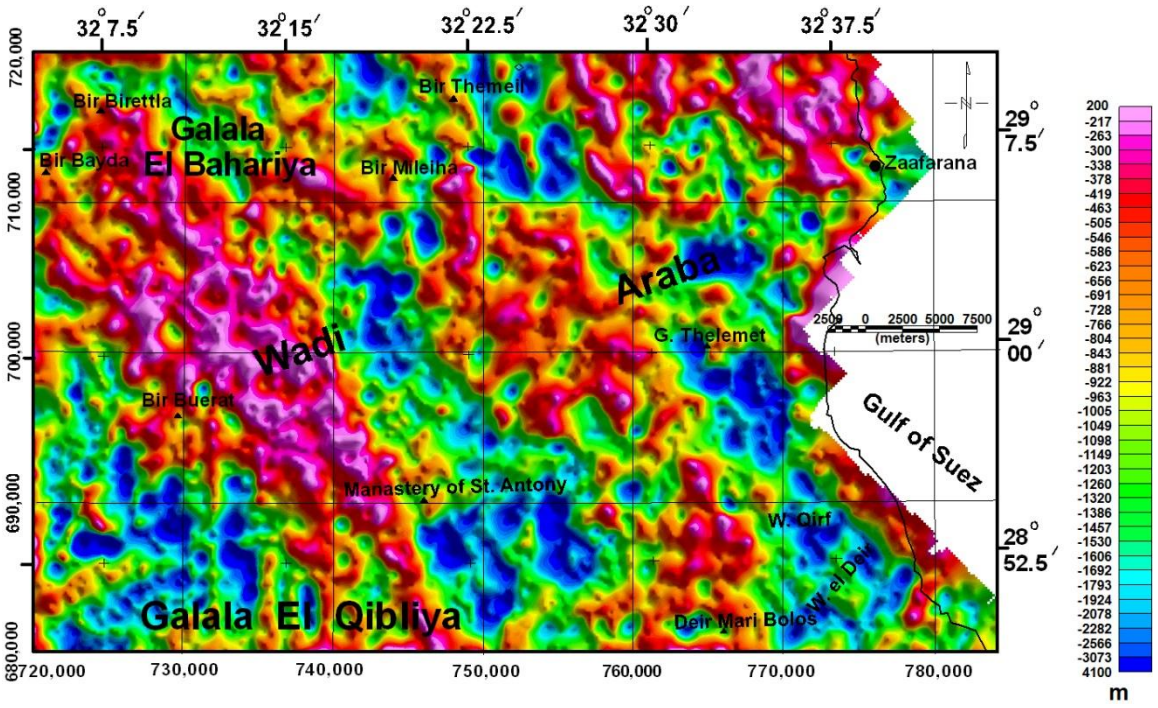

Fig. 11: Depth to magnetic basement calculated by using SPI technique, Wadi Araba.

The TDRwas used to locating the edge of the regional and residual sources. Zero contour line of the TDRrepresents these sources edges. Positive values are assumed to be located above the magnetic sources while negative values are located away from them. The half distance between $\pm\pi/4$ (± 0.785) Radian was used to calculating the edges depths. The calculated depth by this method [21] changes from few hundreds of meters to about 4000m. The THDR_TDR map shows that these edges are much sharper gradientand its values are the reciprocal of the depth to these contacts. The deduced average depths above them varies from about few hundred of meters to more than 4000m.Standard 3D-Euler deconvolution (ED) was carried out on the RTP aeromagnetic data. The suitabledepth solutions are derived by using structural index 0 (contact structural index according to [15], window size of 15x15 and grid cell size 300m. ED is a locator and depth estimator for magnetic contacts under the assumption that the edges of anomalous sources are caused by vertical contacts. Under this assumption the resulted solutions are plotted on the TDR map. A very good correlation between these techniques was introduced. This correlation is an easiest way to confirm the horizontal location and depth of the edges.Both of TDR and ED show that the area is affected by Gulf of Suez rifting system. This can be noticed by the abundance of the NW trends which related to the Gulf rifting systemallover the area especially at the eastern part. The southwestern corner is less affected by this rifting system where deep regional components preserve its older E-W trend which related to the Tethyan or Mediterranean trend.

Two main techniques used to calculate the depth to the magnetic basement sources. AS and SPI reflex a similar results about the basement depths. Form both of them the depth ranges from about 115 m to more than 4000 m.

Finally, the TDR, ED,AS and SPI techniques attributes to delineate the location and depths for edgesof magnetic sources of Wadi Araba area.

References

[1] N. Bournas and H. A Baker, Interpretation of magnetic anomalies using the horizontal gradient analytic signal. *Annali di Geofisica44*, 2001, 506-526

[2] V. E. Ardestani and H. Motavalli, Constraints of analytic signal to determine the depth of gravity anomalies. *Journal of Earth & space physics 33*, 2007, 77-83

[3] M. Arisoy and U. Dikmen, Edge Detection of Magnetic Sources Using Enhanced Total Horizontal Derivative of the Tilt Angle. *Bulletin of the Earth Sciences Application and Research Centre of Hacettepe University 34*, 2013, 73-82

[4] M. Pilkington, P. Keatin, Contact mapping from gridded magnetic data: a comparison of techniques. *Exploration geophysics. 35*, 2004, 206-311

[5] G. R. J. Cooper and D. R. Cowan, Edge enhancement of potential-field data using normalized statistics. *Geophysics, 73*, 2008, 1-4

[6] G. R. J. Cooper, Balancing images of potential field data. *Geophysics, 74*, 2009, 17-20

[7] A. Salem, S. Williams, D. Fairhead, R. Smith and D. Ravat, Interpretation of magnetic data using tilt-angle derivatives. *Geophysics, 73*, 2008, L1–L10

[8] K. A. Salako () Depth to Basement Determination Using Source Parameter Imaging (SPI) of Aeromagnetic Data: An Application to Upper Benue Trough and Borno Basin. Northeast, Nigeria. *Academic Research International, 5*, 2014, 74-86

[9] A. R. Moustafa and M. H. Khalil,. Superposed deformation in the northern Suez Rift, Egypt: relevance to hydrocarbons exploration. *Journal of Petroleum Geology, 18*, 1995, 245-266.

[10] R. Said, *The Geology of Egypt* (Elsevier, Amsterdam, 1962)

[11] J. Kuss, C. Scheibner and R. Gietl, Carbonate platform to basin transition along an Upper Cretaceous to Lower Tertiary Syrian arc uplift, Galala Plateaus, Eastern Desert, Egypt. *Geoarabia 5*, 2000, 405-424.

[12] K. Bandel and J. Kuss, Depositional environment of the pre-rift sediments of the Galala Heights (Gulf of Suez, Egypt). *Berliner geowissenschaftlicheAbhandlungen (A), 78*, 1987, 1–48.

[13] M. H. Shalaby, *Geology and radioactivity of Wadi Dara area, North Eastern Desert, Egypt.* Thesis Ph.D. Alexandria University, 1985.

[14] EGPC (Egyptian General Petroleum Corporation), *Aeromagnetic survey of north Eastern Desert and Gulf of Suez*, by Western Geophysical Company of America, 1983.

[15] Geosoft (Oasis Montaj) Program, *Geosoft Mapping and Application System*. Inc, Suit 500, Richmond St. West Toronto, ON Canada N5SIV6. Users' Manual. 2007.

[16] B. K. Bhattacharyya, Continuous spectrum of the total-magnetic field anomaly due to a rectangular prismatic body. *Geophysics 31*, 1966, 97–121

[18] Y. W. Lee, *Statistical theory of communication*. Willey and Sons, New York, 1960, 1 - 75.

[18] A. Spector and F. S. Grant, Statistical models for interpreting aeromagnetic data. *Geophysics 35*, 1970, 293-302

[19] H. G. Miller and Singh V () Potential field tilt-a new concept for location of potential field sources. Jour of Appl. *Geophysics, 32*, 1994, 213-217

[20] B. Verduzco, J. D. Fairhead, C. M. Green and C. MacKenzie, New insights into magnetic derivatives for structural mapping. *The Leading Edge, 23*, 2004, 116–l19.

[21] A. Salem, S. Williams, J. D. Fairhead, D. Ravat and R.Smith, Tilt-depth method: A simple depth estimation method using first-order magnetic derivatives. *The Leading Edge, 26*, 2007, 1502–l505.

[22] J. D. Fairhead, A. Salem, S. Williams and E. Samson, Magnetic interpretation made easy: The tilt-depth-dip-Δk method. *In2008 Annual International Meeting Expanded Abstracts. Society of Exploration Geophysicists*, 2008, 779–783

[23] W. J. Hinze, R. R. B. Von Frese and A. H. Saad, *Gravity and Magnetic Exploration Principles, Practices, and Applications.* Cambridge University Press, New York, 2013.

[24] A. B. Reid, J. M. Allsop, H. Granser, A. J. Millett and I. W. Somerton, Magnetic interpretation in three dimensions using Euler deconvolution. *Geophysics, 55*, 1990, 80-91

[25] E. E. Klingele, L. Marason and H. G. Kahle, Automatic interpretation of gravity gradiometeric data in two dimensions: vertical gradient. *Geophysical Prospecting, 39*, 1991, 407-434.

[26] L. Marason and E. E. Klingele, Advantage of using the vertical gradient of gravity for 3-D interpretation. *Geophysics, 58*, 1993, 349-355.

[27] E. Harris, W. Jessell, and T. Barr, Analysis of the Euler deconvolution techniques for calculating regional depth to basement in area of complex structures. *SEG Ann. Intern. Meeting*, 1996

[28] P. Y. Stavrev, Euler deconvolution using differential similarity transforms of gravity or magnetic anomalies. *Geophysical Prospecting, 45*, 1997, 207-246.

[29] V. Barbosa, J. Sliva and W. Medeiros, Stability analysis and improvement of structural index in Euler deconvolution. *Geophysics, 64*, 1999, 48-60.

[30] D. Ravat, Analysis of the Euler method and its applicability in environmental investigations. *Journal of Environmental & Engineering Geophysics, 1*, 1996, 229-238.

[31] R. J. Durrheim and G. R. J. Cooper, () EULDEP: A program for the Euler deconvolution of magnetic and gravity data. *Computer & Geosciences, 24*, 1998, 545-550

[32] W. R. Roest, J. Verhoef and M. Pilkington, Magnetic inter-pretation using the 3-D analytic signal. *Geophysics, 57*, 1992, 116-125.

[33] I. N. Mocloed, 3-D Analytic signal in interpretation of total magnetic field data at low magnetic latitudes. *Exploration Geophysics, 24*, 1993, 679 -688.

[34] J. B. Thurston and R.S. Smith, Automatic conversion of magnetic data to depth, dip, and susceptibility contrast using the SPI (TM) method. *Geophysics, 62*, 1997, 807-813.

[35] W. M. Meshref, S. H. Abdel-Baki, H. M. Abdel-Hady and S. A. Soliman, Magnetic trend analysis in the northern part of Arabian Nubian Shieldand its tectonic implications. *Annals of the Geological Survey of Egypt*. 10, 1980, 939-953.

[36] A. R. Moustafaa and O. A. Shaarawy, Tectonic setting of the northern Gulf of Suez. *Geophysical Society of Egypt Bulletin, 5*, 1987, 339-368.

[37] L. Affleck, Magnetic anomaly trend and spacing patterns. *Geophysics, 28*, 1963, 379-395.

[38] D. H. Hall, Magnetic and tectonic regionalization on trxada Island, British Columbia, *Geophysics, 29 (4)*, 1964, 566-581.

[39] M. I. Youssef, Structural pattern of Egypt and its interrelation. *American Association of Petroleum GeologistsBulletin, 52(4)*, 1968, 601-614.

[40] M. Abdel Gawad, No evidence of transcurrent movements in Red Sea area and petroleum implications. *American Association of Petroleum GeologistsBulletin*, 53(7), 1969, 1466-1479.

[41] H. E. El-Shazly, Discrimination of geological features in the Gulf of Suez area using digital and photographic enhancements of

Landsat MSS data. *Egyptian Journal* of *Geology*, 30, 1986, 47-54.

[42] A. S. Abu El Ata, The relation between the local tectonics of Egypt and the plate tectonics of the surrounding regions, using Geophysical and Geological data. *Egyptian Geophysical Society Proceedings of 6th Annual Meeting*, Cairo. 1988.

[43] W. M. Meshref, and E. M. I. El-Kattan, Tectonic pattern of El Qaa plain, Sinai using aeromagnetic data. Proceeding of the 2nd Conference on Geology of Sinai for Development, Ismailia, 1989, 33-48.

[44] B. Oruc, Edge Detection and Depth Estimation Using a Tilt Angle Map from Gravity Gradient Data of the Kozaklı-Central Anatolia Region. Turkey. Pure and Applied Geophysics, Springer, Basel AG 2010, doi: 10.1007/s00024-010-0211-0.